In-situ observations of nucleation in Al-0.1Mg

Wu, G.L.; Ubhi, H.S.; Petrenec, M.; Juul Jensen, Dorte

Published in:
I O P Conference Series: Materials Science and Engineering

Link to article, DOI:
10.1088/1757-899X/89/1/012051

Publication date:
2015

Document Version
Publisher's PDF, also known as Version of record

In-situ observations of nucleation in Al-0.1Mg

2015 IOP Conf. Ser.: Mater. Sci. Eng. 89 012051

(http://iopscience.iop.org/1757-899X/89/1/012051)

In-situ observations of nucleation in Al-0.1Mg

G L Wu[1], H S Ubhi[2], M Petrenec[3] and D Juul Jensen[4]
[1] College of Materials Science and Engineering, Chongqing University, Chongqing, China
[2] Oxford Instruments, Nano Analysis, High Wycombe, HP12 3SE, UK
[3] Tescan Orsay Holdings a.s, Brno, Czech Republic
[4] Danish-Chinese Center for Nanometals, Section for Materials Science and Advanced Characterization, Department of Wind Energy, Technical University of Denmark, Risø Campus, DK-4000 Roskilde, Denmark

E-mail: wugl@cqu.edu.cn

Abstract. A tensile sample of an Al-0.1Mg alloy was in-situ tested in a SEM followed by in-situ annealing to develop recrystallizing nuclei/grains. The evolution of microstructure and crystallographic orientations were characterized using the EBSD technique. Changes in the same area within the sample during deformation and annealing steps were closely followed. During the deformation process the original grains remained recognizable, but became elongated and developed sub-structures. Over the annealing process nuclei with old and new orientations develop at high angle grain boundaries as well as at interior regions with large orientation spreads. Recrystallization twinning was also observed to occur in this Al alloy sample. Furthermore, some localized grain growth during the recrystallization was observed.

1. Introduction

Recrystallizing nuclei form in deformed metals and alloys during annealing. The orientations of nuclei to a large extent determine the final texture of recrystallized metals and alloys [1]. The relationships between the orientations of nuclei and the deformation matrix in which they form are not clear in particular when the large variations in orientations over small distances in the deformed matrix are considered. Classic nucleation mechanisms, predict that the nuclei will have orientations as those present at the matrix sites where they form [2]. It has however also been reported that recrystallizing nuclei with new orientations different from those in the deformed matrix are observed experimentally [3-9]. In most of the above studies, post-mortem analyses were used. One of the difficulties of these studies is that once the nucleation has occurred the pre-existing matrix has disappeared. This is also referred to as the lost evidence problem [10]. Direct characterizations of the microstructural evolution during the nucleation process are rare but considered essential for understanding of the nucleation mechanisms.

Recently, three-dimensional X-ray diffraction microscopy (3DXRD) was used for characterization of nucleation in 3D. Both Cu and Al samples were studied in this way [11, 12]. In both experiments nuclei with new orientation were observed. This type of experiment does not suffer from the lost evidence problem. However, the spatial resolution of those 3DXRD experiments was limited so the deformed microstructures could not be well resolved. Only the orientation distributions in the deformed materials were precisely determined. Another disadvantage of the 3DXRD is the restricted

access to synchrotron sources so that only few experiments are possible. Therefore in the present work we have used in-situ heating in a scanning electron microscope (SEM) coupled with electron backscatter diffraction (EBSD) measurements for in-situ studies of nucleation with the aim of pin-pointing nucleation sites and orientation relationships between nuclei and parent matrix. Such in-situ measurements have been used before fore recrystallization studies, e.g. Ref. [13-18]; new in the present work is that we also follow the deformation in-situ before the annealing.

2. Materials and methods

The material used in the present study was a fully annealed 2mm thick Al-0.1%Mg rolling sheet. A dog bone tensile sample with a gauge size 2mm long and 2mm wide was cut from the sheet, with the tensile direction (TD) of the sample being parallel to the transverse direction of the rolling sheet. The tensile sample was ground to 4000 grit SiC paper followed by electropolishing in a perchloric acid based solution. Then the sample was mounted in a TESCAN MIRA XM FEGSEM using a GATAN Microtest EH2000EW in-situ tensile and heating stage. The SEM was equipped with an Oxford HKL NordlysMax EBSD detector for microstructure characterization. The clippers of the in-situ stage were 70° pre-tilted so that the normal surface of the sample (containing TD and short transverse direction, SD, perpendicular to the normal direction, ND) to be analyzed by EBSD was 20° aligned to the phosphor screen of the EBSD detector. Tensile elongation was driven and controlled by a step motor. Two heating elements were mounted on the clippers of the stage with one element on each clipper. The sample was heated directly by heat conduction from the heating elements by an electric current.

An area approximately at the center of the tensile sample was first characterized by EBSD. Then the sample was elongated to a true strain of about 0.58 in 8 steps at room temperature. During the in-situ tensile test, the scanned area was elongated along the tensile direction and was compressed perpendicular to the tensile direction. The corresponding area was characterized by EBSD after each tensile step so that the evolutions of microstructure and orientations of the individual grains within the area were followed in-situ. Then, the sample was heated to 290℃. It took about 30 minutes to reach 290℃. After collecting an EBSD scan of the selected area, the sample was held at 290℃ for 1 hour. EBSD scans were obtained every 10 minutes of the same area to follow the microstructural evolution during the in-situ annealing. Finally, the recrystallizing grains were detected from the EBSD maps by the DGR method [19]. The recrystallizing grains detected in the first two annealing steps (i.e. heated to 290℃ and hold for 10 minutes) were considered as recrystallization nuclei and are analysed in the present work.

3. Results and Discussion

3.1 Initial microstructure

Figure 1a shows the initial microstructure of the area that was followed during the in-situ tensile deformation. The area is 550μm by 1mm. The average grain size is about 90 μm. The initial texture as shown by the pole figure consists of cube, {001}<100>, and rotated Goss, {110}<011>, orientations.

3.2 Evolutions of microstructure and orientations during in-situ tensile test

Figure 2a shows the microstructure after step 4 (corresponding to a true strain of 0.33). Most of the initial grains can be recognized. Low angle dislocation boundaries are formed within the grains. Some grains develop relatively large local orientation variations. In a few areas, the microstructures cannot be resolved due to poor pattern quantity caused by large local plastic deformation and severe surface relief. Figure 2b shows that cube grains have large orientation spreads and relative small overall lattice rotations, whereas the Goss grains rotated about one of {111} poles so that they developed relative small orientation spreads but large lattice rotations.

Figure 3a shows the microstructure after in-situ tension to a true strain of 0.58. Although many areas cannot be resolved by EBSD due to local plastic deformation and surface roughing, some initial grains can still be recognized. Figure 3b shows the corresponding pole figure. As compared to the pole

figure after deformation to 0.33 in Fig. 2b, it is seen that all the grains developed large orientation spreads and small overall lattice rotations during the tensile deformation from 0.33 to 0.58.

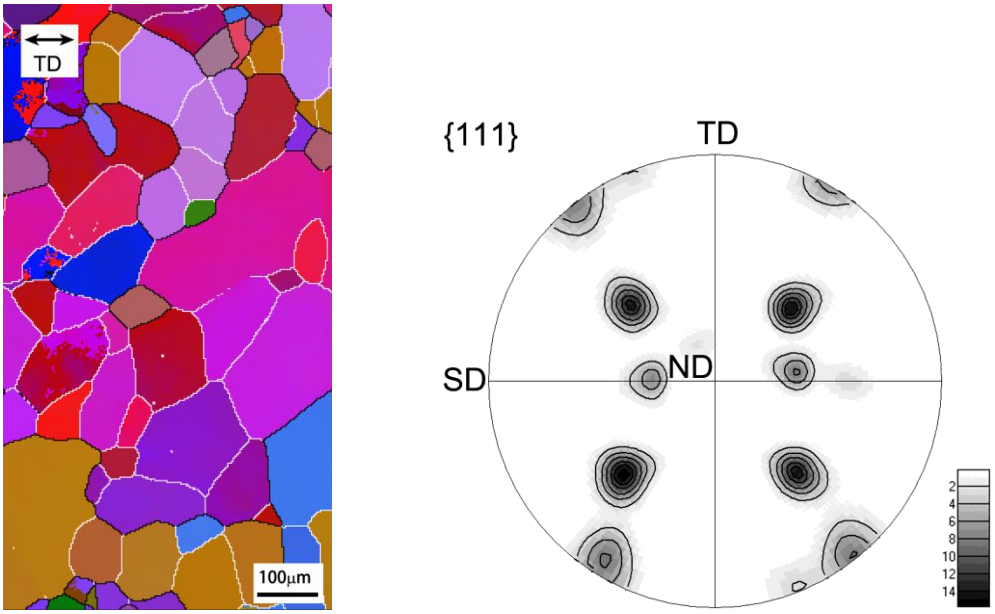

(a) **(b)**

Figure 1. (a) The initial microstructure and (b) the initial texture of the area to be followed during the in-situ tensile deformation. In the EBSD map, white and black lines represent grain boundaries $\geqslant 2^\circ$ and $\geqslant 15^\circ$, respectively. The colours of the EBSD map are so-called Euler colours, in which the three Euler angles by Bunge notion for the orientation of each datapoint are coloured by red, green and blue, respectively.

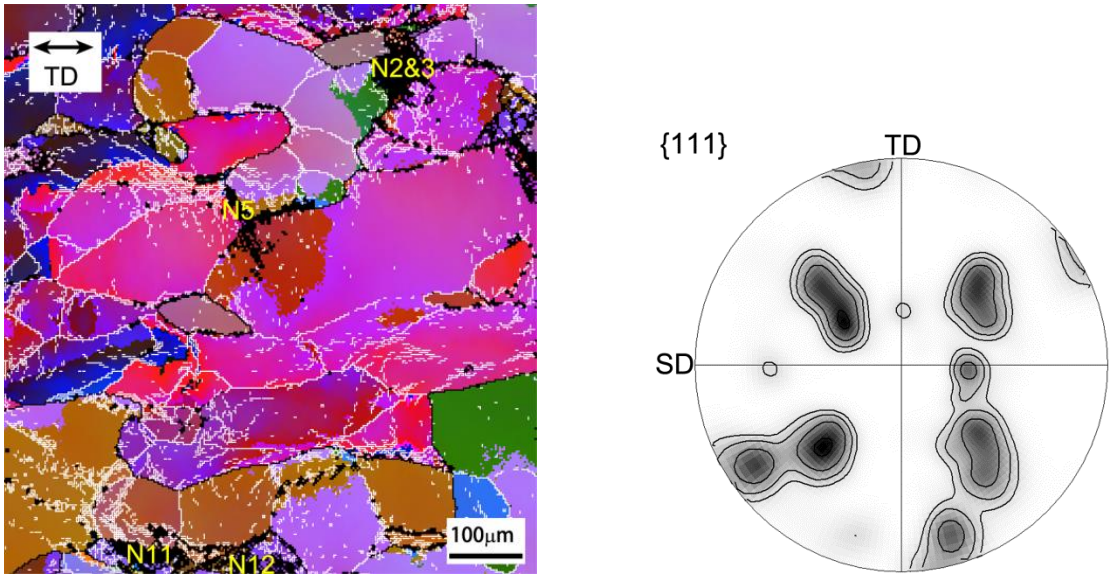

(a) **(b)**

Figure 2. (a) EBSD map and (b) {111} pole figure after in-situ deformation to 0.33. In the EBSD map, the black pixels are non-indexed data points. Some positions where nuclei are found to develop upon annealing are numbered by N_i. The intensity levels in the pole figure are as in Fig. 1b.

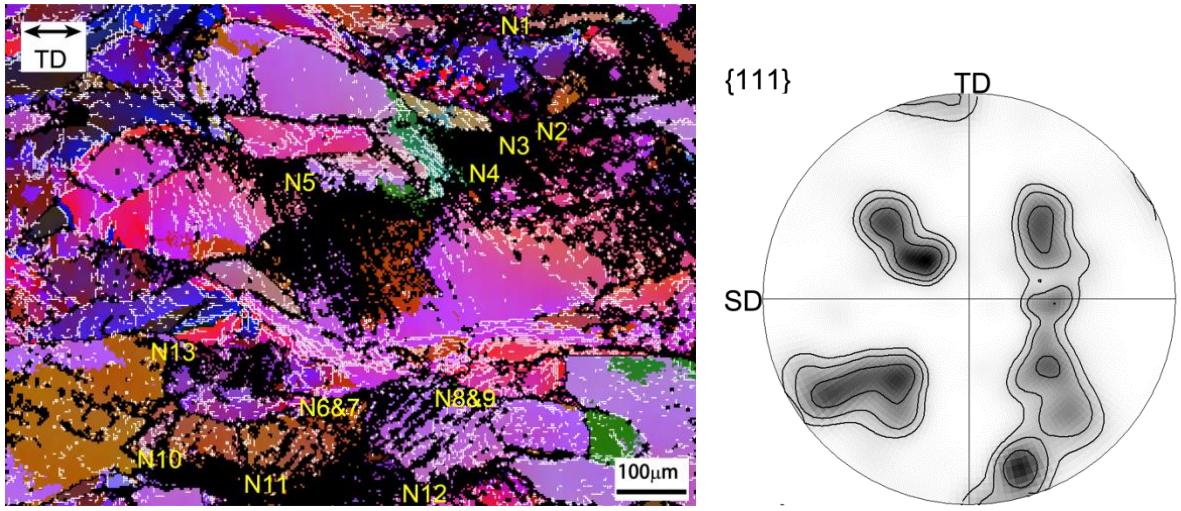

(a) **(b)**

Figure 3. (a) EBSD map and (b) {111} pole figure after in-situ deformation to 0.58. The positions where nuclei are found to develop upon annealing are numbered by N_i. The intensity levels in the pole figure are as in Fig. 1b.

3.3 Evolutions of microstructure and orientation during in-situ annealing.

Figure 4a and 4b show the microstructures after the sample has been heated to 290℃ and being held at the temperature for 10 minutes, respectively. In the area, 13 recrystallization nuclei can be clearly identified. All the nuclei sites are marked in Fig. 4. After carefully tracking the grain structure during the in-situ tensile test, the nucleation sites of all the nuclei were successfully determined in the original structure and subsequent tensile steps (see Figs.2 and 3). It is seen that all nuclei are formed at areas inside the original grains associated with large deformation or at original grain boundaries.

Grain boundaries are thus confirmed to be effective nucleation sites during annealing for nucleation in agreement with many previous observations [e.g. 20]. In interior areas with large localized plastic deformation which are also found to be potential nucleation sites in the present work, the lattice rotation and/or lattice curvatures are large and thus the local orientation spreads are also large. High deformation energy will therefore be stored in these areas, which will facilitate the formation of nuclei.

After comparing the orientations of the nuclei to the orientations in the deformed matrix where they developed (as shown in Fig. 3a), it is found that 8 nuclei have orientations fully within the orientation spread of the deformed matrix or their misorientations to the deformed matrix are smaller than 20°.These orientations are considered to have “old orientations”, already presented at these sites in deformed structures. The reason why deviations as large as 20° are included for nuclei of old orientations is that in certain areas the EBSD pattern quality is low with many non-indexed pixels. So the 20° deviation is accepted and is considered a conservative criterion. Even applying this conservative criteria, there are 6 (N2, N3, N5, N6, N11 and N12) nuclei with misorientations to the deformation matrix greater than 20° (i.e. with “new orientations”). It is found that the nucleation sites of five of these six nuclei with new orientations are interior areas with large local deformation, where the EBSD pattern qualities are comparable low. The nucleation sites for these 5 nuclei are therefore also marked in Fig. 2a.

Figure 5a shows the pole figure of the nucleus N6. N6 is about 45°<110> misoriented to one of its parent deformed grains. However, it is found that there is a thin twin to the right of N6 (indicated by the arrow). The twin of N6 is 59°<433> misoriented to the deformed grain. Like N6, the tiny grain to the right of N5 (indicated by the arrow) is also twin related to the deformed grain. Therefore, it is plausible that N5 and N6 are formed by twinning during annealing. Figure 5b shows the pole figure of

the nucleus N3 and its deformed parent grains. The misorientation between N3 and the pixels near the nucleation site in the deformed grains are approximately 42°<343>, 31°<340> and 25°<110>, respectively. It is seen that the nucleus has a ~40°<111> misorientation to the deformed grain lying to the right of the nucleus. Similarly, N2, N11 and N12 also have a ~40°<111> misorientation relationships to their parent deformed grains.

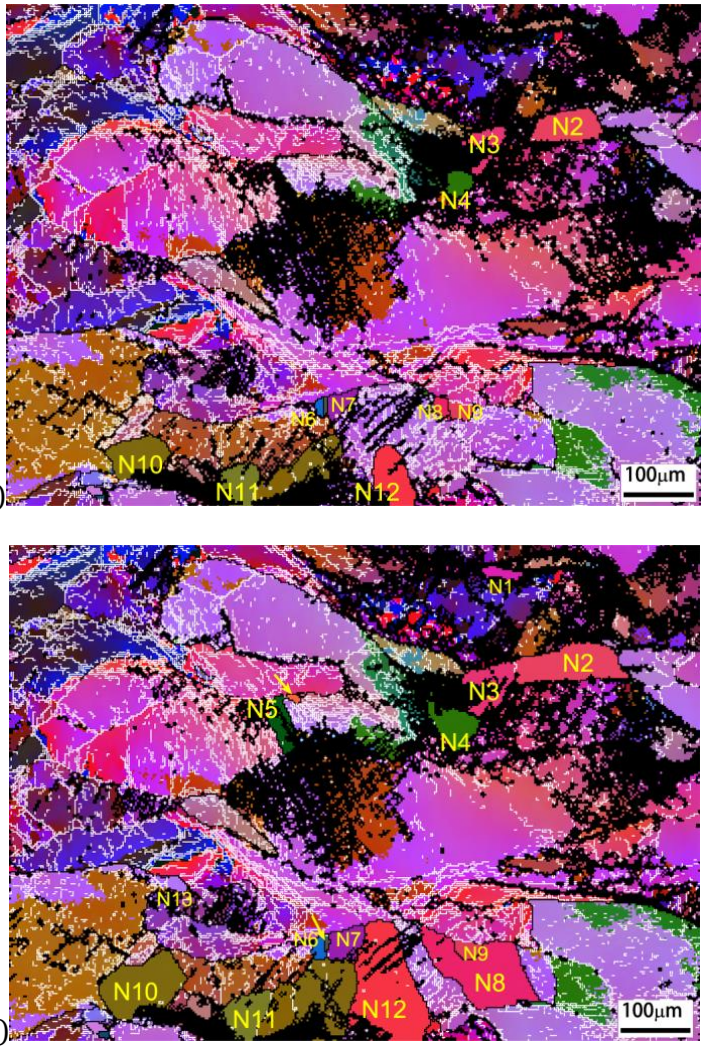

Figure 4. EBSD maps of the selected area after the sample was (a) heated to 290℃ and (b) hold at 290℃ for 10 minutes.

For the local areas in the deformed parent grains leading to the formation of nuclei, the average orientation spreads of the areas at nucleation sites (expressed by the average misorientation angle between each data point within the area and the mean orientation of the area) were calculated. It is found that areas/grains with small orientation spreads only form nuclei with old orientations. Grains having large orientation spreads may also form nuclei with old orientations. However, deformed areas/grains developing nuclei with new orientations all show large orientation spreads. It should be noted that especially in these areas many pixels on the EBSD map were not indexed and the local orientation spreads are therefore expected to be even larger than that measured.

Although most of nuclei were found to have old orientations, there are 4 nuclei which are neither twin-related to the deformed matrix nor close to the orientations within deformed parent grains. Nuclei with old orientations may just develop in the deformed parent grains with small orientation spreads by

the processes such as subgrain growth, since the sizes of subgrains are normally large in these areas. The original grain boundaries will promote the growth of the subgrains due to high mobility of the high angle boundaries between the subgrains across the original grain boundaries. Concerning the formation of nuclei with new orientations, the 40°<111> misorientation relationship seems to dominate in the present work. However, the statistic is weak and also the lack of knowledge about what is going on below the investigated surface holds us from further analysis of such misorientation relations based on the present data.

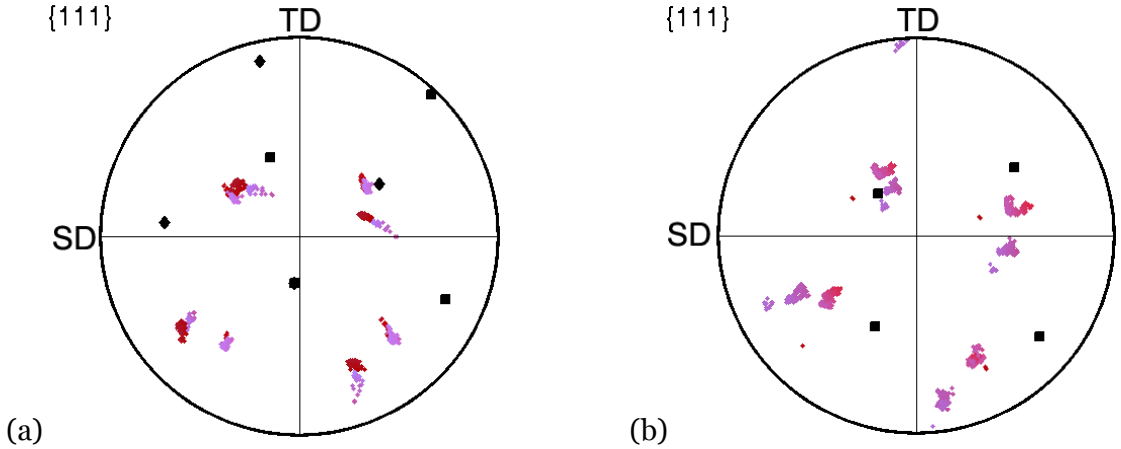

Figure 5. Pole figures of (a) N6 and (b) N3 and the pixels at the nucleation sites in their deformed parent grains. The squares represent orientations of the nuclei, diamonds twins, and colour points deformed grains. The colours in the pole figures are the same as in the EBSD maps.

Annealing twins are often observed in Ni and Cu due to the low stacking fault energies. However, annealing twinning has also been observed in Al [12] with high stacking fault energy although less frequently. In the present work twinning are observed for nuclei N5 and N6. It cannot be determined whether these twins were formed directly from the deformed matrix or from an already existing recrystallizing nucleus/grain. But one interesting point is that these twins (having twin orientation relationship to the deformed matrix) are very small and are observed to be consumed by their neighbouring grains during subsequent annealing; and after complete recrystallization these twins have disappeared. For example, Fig. 6a and 6b show the EBSD maps of grains near N5 after annealing at 290℃ for 30 minutes and 40 minutes, respectively. After annealing for 30 minutes, N5 and the grain twin-related to its deformed parent grain (indicated by the arrow in Figs 4b and 6a) are seen. However, the twin disappeared after annealing for 40 minutes. From the morphologies of the grain boundary between N5 and its neighbouring grain after annealing for 30 minutes and 40 minutes, it is likely that the twin was consumed by the neighbouring grain. These results emphasize that in-situ annealing is an important method to understand nucleation mechanisms, as even more evidence may be lost than just the deformed matrix.

By following the microstructural evolution during all in-situ annealing steps, it is also possible to identify the growth of individual nuclei. It is found that N9 was consumed by N8 after annealing at 290℃ for 40 minutes, at which state the material is only partly recrystallized and N8 and N9 are both partly surrounded by the deformed matrix (see Fig. 7). It is seen in Fig. 4b that the grain boundary between N8 and N9 was highly curved. The curvature might have contributed to the growth of N8 into N9, and it may be concluded that some localized grain growth is also possible during recrystallization in the present material (also see the example shown in Fig. 6).

It may be argued that recrystallization observed by the surface inspections as the present in-situ annealing study, might be different from the bulk behaviour. This of course cannot be ruled out. However, it is at least reassuring that the orientations of the recrystallizing nuclei/grains measured on the surface in the present work are similar to those determined in bulk.

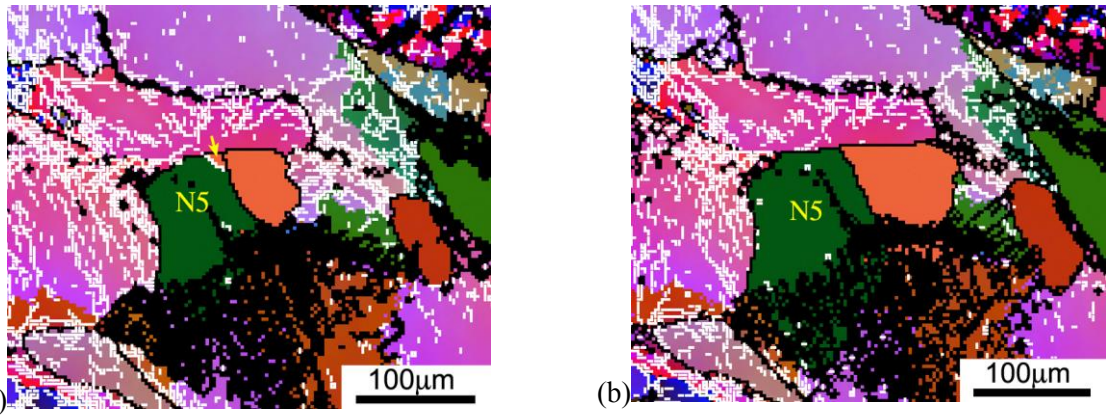

Figure 6. EBSD maps of N5 after annealing at 290℃ for (a) 30 minutes and (b) 40 minutes.

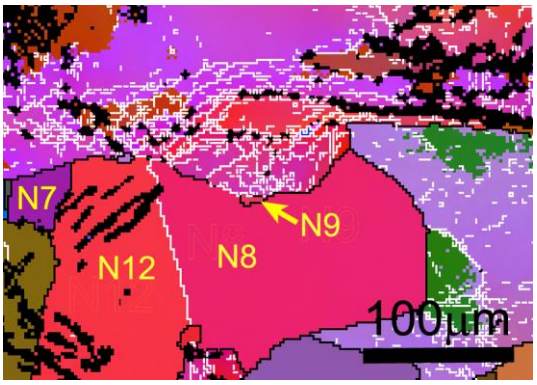

Figure 7. EBSD map of N8 and N9 after annealing at 290℃ for 40 minutes. The grain N9 is indicated by the arrow in the map.

For the studies of recrystallization nuclei, most published results are based on statistic investigations of deformed and annealed samples. The whole deformation history is thus generally not followed. The deformation history including the lattice rotation of grains and the strain accommodation across grain boundaries may influence the nucleation process. In this sense, the in-situ tensile and heating offers an excellent opportunity to follow the microstructural evolution leading to nucleation, which will be analysed in a future study of the present experiment.

4. Conclusions

An Al-0.1Mg alloy sample was in-situ tensile strained to a true strain of 0.58 and then in-situ annealed at 290℃ for 1 hour in a SEM. EBSD was employed to characterize the microstructure and local orientations within the same area on the surface of the sample during the in-situ deformation and annealing processes. After annealing for 10 minutes recrystallizing nuclei/grains developed at original grain boundaries and within interior grain areas with large orientation spreads. Most of the nuclei were found to have orientations close to the orientations within the parent deformed grains and preferentially form at original grain boundaries between grains with relative small local orientation spreads. Nuclei with orientations not observed in the deformation matrix were also detected. These nuclei formed at interior sites with large local orientation spreads. Recrystallization twins were also found in the Al-0.1Mg alloy. The twins, at least for the two cases in the present results, were observed to disappear during the subsequent recrystallization process. Furthermore some localized grain growth was observed to occur before the sample was completely recrystallized due to highly curved grain boundaries. Although the formation of nuclei with new orientations cannot be analysed in detail in the

present results, the present in-situ deformation and annealing experiments provide a powerful approach to study nucleation mechanisms.

Acknowledgments
Financial supports from the National Natural Science Foundation of China (NSFC, Grants No.51471039, 51327805 and 51421001) and Fundamental Research Fund of Central Universities of China (Grant No. CDJZR14135502 and 10611205CDJZXZ138802) are gratefully acknowledged. The authors would also greatly thank the supports from Danish National Research Foundation (Grant No. DNRF86-5) and NSFC (Grant No. 51261130091) to the Danish-Chinese Center for Nanometals.

References
[1] Doherty R D, Hughes D A, Humphreys F J, Jonas J J, Juul Jensen D, Kassner M E, King W E, McNelly T R, McQueen H J and Rollet A D 1997 *Mater. Sci. Eng.* **A 238** 219-74
[2] Humphreys, F J and Hatherly M 2003 *Recrystallization and phenomena 2nd edition*, Oxford, UK, ELSEVIER
[3] Barrett C S 1940 *Trans. AIME.* **137** 128
[4] Beck P A, Sperry P R and Hu H 1950 J. *App. Phy.* **21** 420-25
[5] Inoko F and Miga G 1987 *Scripta Metall.* **21** 1039-1045
[6] Paul H, Driver J H, Maurice C and Jasieński Z 2002 *Acta Mater.* **50** 4339-55
[7] Sabin T J, Winther G and Juul Jensen D 2003 *Acta Mater.* **51** 3999-4011
[8] Okada T, Huang X, Kashihara K, Inoko F and Wert J A 2003 *Acta Mater.* **51** 1827-39
[9] Wu G L and Juul Jensen D 2007 *Acta Mater.* **55** 4955-64
[10] Chung C Y and Duggan B J 1996 *Proc. of 11th Inter. Conf. on Texture of Mater*. (Xi'an, China) 399-404
[11] Larsen A W, Poulsen H F, Margulies L, Gundlach C, Xing Q F, Huang X and Juul Jensen D 2005 *Scripta Mater.* **53** 553-7
[12] West S S, Winther G and Juul Jensen D 2011 *Metall. Mater. Trans.* **42A** 1400-8
[13] Humphreys F J and Ferry M 1996 *Mater. Sci. Forum.* **217** 529-34
[14] Springer F and Radomski M 1997 *Mater. Sci. Forum.* **273** 497-502
[15] Lens A, Maurice C and Driver J H 2005 *Mater. Sci. Eng.* **A 403** 144-53
[16] Nakamichi H, Humphreys F J and Bate P S 2007 *Mater. Sci. Forum.* **550** 441-6
[17] Bozzolo N, Jacomet S and Logé R E 2012 *Mater. Charact.* **70** 28-32
[18] Kerisit C, Logé R E, Jacomet S, Llorca V and Bozzolo N 2013 *J. Microscopy*. **250** 189-99
[19] Wu G L and Juul Jensen D 2008 *Mater. Charact.* **59** 794-800
[20] Vandermeer R A 1995 *Proc. of 16th Risø Inter. Symp. on Mater. Sci.* (Roskilde, Denmark) 193-245